Tribol Lett (2017) 65:115
DOI 10.1007/s11249-017-0898-5

ORIGINAL PAPER

A Combined QCM and AFM Study Exploring the Nanoscale Lubrication Mechanism of Silica Nanoparticles in Aqueous Suspension

B. Acharya[1] · M. Chestnut[2] · A. Marek[2] · A. I. Smirnov[2] · J. Krim[1]

Received: 21 May 2017 / Accepted: 25 July 2017 / Published online: 4 August 2017

Abstract Addition of nanoparticles to liquid lubricants often leads to a reduction in both friction and wear rates for a wide range of solid–liquid–nanoparticle combinations. While the lubricating properties of nanoparticles are well documented, the detailed physical mechanisms remain to be fully explored. In a step toward such an understanding, the nano-tribological properties of gold surfaces immersed in aqueous suspensions of negatively charged SiO_2 nanoparticles were examined by means of Quartz Crystal Microbalance (QCM) and Atomic Force Microscopy methods. The SiO_2 nanoparticles were found to reduce the resistance to shear motion at the QCM's solid–liquid interface. The effect was observed to be concentration dependent, with ca. 1.5 wt% yielding the maximum reduction in shear. An electrokinetic mechanism is proposed whereby the loosely bound nanoparticles roll and/or slide on the surface, while upper layers of nanoparticles slip over the surface layer because of the repulsive electrostatic forces between the individual particles. The nanoparticles were observed to remove the electrode material from the gold surface and slightly increase the overall roughness with the major change happening within the first hour of the exposure. This study inherently provides insight into a complex interface of solid, liquid and nanoparticles at a nanometer scale.

Keywords QCM · Nanoscale roughness · Nano-additives · AFM · Fractal · SiO_2 · Electrokinetic phenomena

1 Introduction

The evolution of lubricant additives has a long history starting from a basic viscosity modifier to the current state of advanced hi-tech formulations to achieve friction reduction, anti-wear, antioxidant and heat transport, etc. [1]. With the ever-increasing sophistication of modern machinery, including smaller sizes, higher fit tolerances, more moving parts and higher efficiency requirements, demands on the additives' performance are accelerating. The new additives ideally should also be biodegradable and environmentally friendly. These concerns among tribologists and lubrication engineers have triggered a growing interest in aqueous suspensions of nanoparticles as a possible solution that is both environmentally friendly and effective.

Prior studies of tribological properties of nanoparticles (NPs) have revealed their potential as highly effective lubricant additives [2]. The small size (<100 nm) of NPs eases their entrance into the contact region and even between the nanoscale asperities making the NP additives effective in all the regimes of lubrication, including the most important boundary lubrication regime. In a recent review, Dai et al. [2] compiled an extensive list of dozens of promising nano-additives composed of metals, oxides, sulfides, carbon derivatives and nano-composites. The major lubrication mechanisms of the nano-additives are: a change in the frictional mode (e.g., by rolling of

✉ B. Acharya
bachary@ncsu.edu

[1] Department of Physics, North Carolina State University, Raleigh, NC 27695, USA

[2] Department of Chemistry, North Carolina State University, Raleigh, NC 27695, USA

nanospheres), a tribofilm formation by tribochemical reactions and/or material transfer, and surface mending/polishing, etc. These very promising but initial results warrant further investigations of tribological phenomena for solid–liquid–nanoparticle combinations.

The Quartz Crystal Microbalance (QCM) is an elegant tool for exploring interfacial effects on the nanoscale. It has been widely used as a nano-tribological technique for studying uptake and sliding of adsorbed films in both vacuum [3] and liquids [4], including the effects of additives. The characteristic oscillating frequency of QCM on the order of ca. 10 MHz and the amplitude of mechanical oscillations on the order of tens of nm correspond to sliding speeds of tens of cm/s that overlap with typical sliding speeds employed by macroscale tribotesters. The QCM is specifically beneficial for the study of solid–liquid–nanoparticle interfaces in the absence of a counter-surface to understand how nanoparticles interact with surfaces when dispersed in liquids and how they impact shear resistance to motion at solid–liquid interfaces.

Tribological properties of SiO_2 nanoparticle suspensions have to date been studied in a wide range of liquids (water, ethylene glycol, paraffin and other base oils) [5–8]. These studies reported that SiO_2 nanoparticles are easily accessible, environmentally clean (relative to organic lubricant additives), eco-friendly and have a good dispersity and stability in those solvents. They moreover result in reduced friction and surface wear levels at certain concentrations. The proposed lubrication mechanism is generally thought to be film formation at the contacting interfaces, allowing for a higher load bearing capacity while reducing the direct contact between the interfaces. Concentration-dependent reductions in friction coefficients of up to 25% have been reported in these prior studies that diminish and/or disappear after exceeding a threshold particle concentration level [6, 8]. These phenomena are somewhat counterintuitive, as one might expect NPs at higher concentrations to form thick films on surfaces that would readily de-aggregate even if the NP at higher concentrations had formed fractal aggregates in the suspension [9]. It is therefore important to investigate how that mechanism correlates with the nanoscale effects at the solid–liquid–nanoparticle interface.

In this study, nano-tribological properties of commercial amorphous colloidal silica with the specified size of 60 nm and dispersed in water have been investigated by monitoring shifts in the resonance frequency and the motional resistance (dissipative property) of QCM crystals plated with gold surface electrodes. The surface electrodes were then examined with Atomic Force Microscopy (AFM) for any changes in the texture and roughness, etc., in order to assess possible polishing/mending effects.

2 Materials and Methods

2.1 Preparation and Characterization of SiO_2 Nanosuspensions

Silicon dioxide (silica) nanoparticles were obtained from Buehler (a division of Illinois Tool Works (ITW), Lake Bluff, IL) as a MasterMet® silica colloidal dispersion in water. The dispersion was specified to be composed of 50–60 nm silica particles at pH $\approx$ 10. The dispersion was either used as received or diluted with deionized water (pH = 6.75) for further characterization.

Distribution of the particles' hydrodynamic size as well as zeta potentials were determined using dynamic light scattering (DLS, Zetasizer, Malvern, Westborough, MA) upon dilution of the original stock suspension with deionized water. pH of the diluted suspensions was monitored by a VWR Symphony SB70P pH meter (VWR International, Radnor, PA). Table 1 summarizes DLS and zeta potential data together with pH measurements for the dilution series. For typical dilutions of 1:50, the average diameter by number was $d = 66 \pm 20$ nm and the particles were negatively charged with zeta potential $\zeta = -40.6 \pm 1.6$ mV. It is notable that the diluted suspensions were not observed to be comprised of NP aggregates, despite the fact that they were diluted from highly concentrated stock suspensions.

Thermogravimetric analysis (TGA, Q50, TA Instruments, New Castle, DE) was employed to determine the concentration of silica NPs in the stock suspension (42.64 wt%). The initial drop of mass to 42.64 wt% was completed at 150 °C with only 0.60 wt% of additional weight loss observed upon heating to 495 °C (data are not shown), that is likely related to a thermal decomposition of hydroxides. This essentially flat TGA response above 150 °C demonstrated no measurable presence of organic impurities in the commercial silica suspension.

The morphology of silica NP dispersed on the surface of QCM electrodes has been further examined by scanning electron microscopy (SEM) using a FEI Verios 460L (FEI Company, Hillsboro, OR) field-emission scanning electron microscope (FESEM) installed and operated by an Analytical Instrumentation Facility (AIF, NCSU). Figure 1 shows a typical SEM image of SiO_2 nanoparticles on a QCM substrate that demonstrates a spherical morphology.

2.2 QCM Measurements

The QCM crystals used in this work were 1″ diameter AT-cut (transverse shear mode, type **A** Temperature compensated), 5 MHz crystals with a 0.5″ diameter gold sensing electrode (Fil-tech, Inc., Boston, MA). Data were collected using a QCM100 (Stanford Research Systems, Sunnyvale,

Table 1 Characterization of SiO_2 nano-dispersion by dynamic light scattering upon dilution with DI water at pH = 6.75 including pH, zeta potential, standard deviation of the mean zeta potential, zeta potential deviation, standard deviation of zeta potential deviation, number average hydrodynamic radius, R_n, standard deviation of R_n, volume average hydrodynamic radius, R_v, standard deviation of R_v, and the polydispersity index (PDI) calculated according to ISO 22412

Dilution	pH	Zeta potential (mV)	Std. (mV)	Zeta potential dev. (mV)	Std. (mV)	R_n (nm)	Std. (nm)	R_v (nm)	Std. (nm)	PDI
1:1	9.44	−8.7	1.7	–	–	17	11	581	445	0.889
1:20	9.41	−6.4	0.9	19.3	4.0	17	3	143	38	0.326
1:50	9.08	−40.6	1.6	12.5	3.2	33	10	232	162	0.278
1:100	8.9	−39.0	1.0	11.5	1.8	37	4	233	68	0.228
1:250	8.42	−38.2	1.6	7.8	1.1	37	2	166	35	0.207
1:500	8.02	−34.5	1.4	14.9	4.4	38	2	182	108	0.214
1:1000	7.27	−32.7	0.9	14.0	2.8	39	2	131	60	0.196

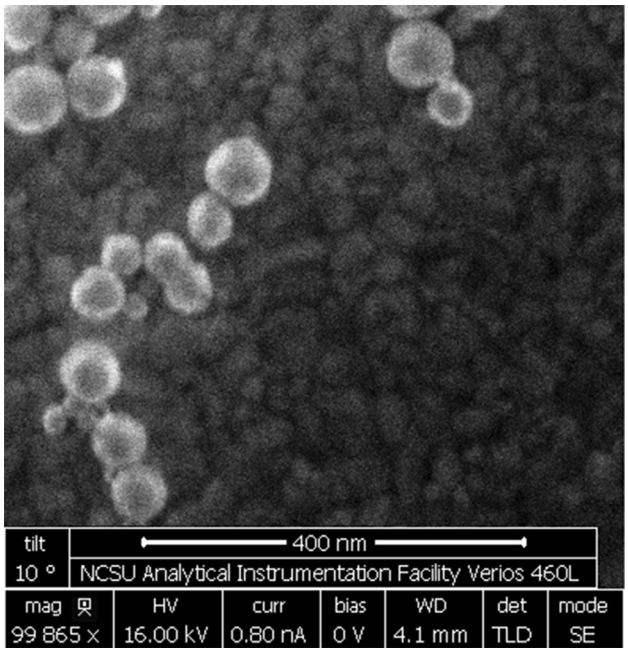

Fig. 1 A typical SEM image of SiO_2 nanoparticles on a QCM substrate

CA, USA) system comprised of an oscillator driving circuitry, a controller and a Teflon holder. The frequency and conductance of the crystal were measured by a frequency counter (HP 53181A, Keysight Technologies, Santa Rosa, CA) and a multimeter (Keithley 2000 Series, Tektronix, Inc., Beaverton, OR), respectively. The conductance, initially measured in volts, was converted to motional resistance of the QCM using the relation $R = 10^{4-V/5} - 75$ [10], where V is the conductance in volts and R is the motional resistance of QCM in Ohms. Changes in the motional resistance of a crystal are directly proportional to changes in the inverse quality factor, as will be described in Sect. 2.3. A LabVIEW program (LabVIEW 7.1, National instruments, Austin, TX) recorded the frequency and conductance of the crystal at 5 s intervals.

The QCM crystal was mounted vertically and then immersed into a cell containing about 60 ml of deionized (DI) water so that only the surface electrode side was in a contact with the liquid. Typically, a few ml of SiO_2 NP stock was then added to the cell thereby obtaining a desired NP concentration (from 0.5 to 1.75 wt% of SiO_2). The QCM experiments were conducted for either 1 or 24 h. All measurements were taken at room temperature. After completing the measurement in the NP suspension, the crystal was removed from the suspension, rinsed with DI water, and allowed to dry in ambient air while continuing data recording. This procedure helps to identify whether the net mass of the QCM increases (via attachment of NPs) or decreases (through the electrode erosion by NPs). Physically adsorbed NPs are expected to be readily removed after a water rinse while chemically bound NP's are not. The rinsed QCM gold surface was also examined by AFM as described in Sect. 2.4.

The initial QCM experiments were carried out by varying NP concentrations from 0.5 to 1.75 wt% SiO_2 in water in 0.25 wt% increments. The optimal reduction in shear resistance to motion was observed at 1.5 wt%. The experiments at the optimal concentration were performed four times, and only minor deviations were observed between the individual runs.

2.3 QCM Data Analysis

A QCM crystal reflects any change in the environment surrounding its surface electrodes via changes in the resonant frequency, δf, and the inverse quality factor, $\delta(Q^{-1})$. The δf and $\delta(Q^{-1})$ parameters relate to the frictional energy losses of materials deposited onto the surface electrodes and/or drag forces and interfacial slippage of fluids in which the crystal is immersed. When a QCM is immersed in a fluid of density ρ and viscosity η, the δf and $\delta(Q^{-1})$ associated with an increased inertia and additional viscous drag forces of the oscillator, under no-slip boundary conditions, are given by [11]:

$$-\frac{\delta f}{f_0} = \frac{\delta(Q^{-1})}{2} = \sqrt{\frac{\rho\eta f_0}{\pi\rho_q\mu_q}} \quad (1)$$

where f_o is the frequency of unloaded crystal in air, $\rho_q = 2.648$ g/cm^3 is the density, and $\mu_q = 2.947 \times 10^{11}$ g/cm/s^2 is the shear modulus of quartz.

Since the viscous drag forces on the QCM electrode are mechanical in nature, a decrease in quality factor represents an increase in the series resonant resistance R of the QCM resonator that can be measured electrically. Martin et al. [12] formulated the relation for the change in the motional resistance of QCM with its surface electrode exposed to a fluid from one side under non-slip conditions to be:

$$\delta R = \frac{1}{8K^2C_0}\sqrt{\frac{\pi\rho\eta}{f_0\rho_q\mu_q}} \quad (2)$$

where $K^2 = 7.74 \times 10^{-3}$ is the electromechanical coupling factor for the AT-cut quartz and C_0 is the static capacitance of the QCM electrodes.

For the QCM crystals employed here ($f_o = 5$ MHz), the theoretical values for δf, $\delta(Q^{-1})$ and δR for one side immersed in water at 20 °C are approximately −715 Hz, 2.85×10^{-4} and 300 Ω, respectively. However, in practice, the observed shifts upon an immersion of QCM into a liquid are larger than those predicted by Eqs. (1) and (2), primarily because of roughness of the QCM surface electrode [13–15]. Surfaces with higher roughness will have higher shifts in the frequency and motional resistance. This effect has been found to be observable even for surfaces with root mean square (rms) roughness as small as 1 nm [16].

When a QCM electrode encounters dispersed NPs, the latter may adhere rigidly or loosely to the surface or change the surface roughness characteristics, thus, causing some further change in both resonant frequency and quality factor of the QCM. As originally reported by Sauerbrey [17], an additional rigidly adhering film deposited onto one side of a QCM will decrease its resonant frequency by:

$$\delta f_{\text{film}} = -\left(\frac{2f_0^2}{\sqrt{\rho_q\mu_q}}\right)\left(\frac{m_f}{A}\right) = -2.264 \times 10^{-6}\left(\rho_2 f_o^2\right), \quad (3)$$

where $\rho_2 = (m_f/A)$ is the mass per unit area of the film in g/cm^2.

For one layer of 60-nm-diameter spherical SiO_2 nanoparticles packed in the closest hexagonal arrangement (assuming SiO_2 bulk density of 2.65 g/cm^3, yielding $\rho_2 = 9.6 \times 10^{-6}$ g/cm^2) adhering rigidly atop of a 5 MHz QCM, the resulting frequency shift is $\delta f_{\text{film}} = -544$ Hz using Eq. (3) assuming an uptake of the particles on the surface, with no associated shift in Q. If, however, the slip conditions at the boundary change upon the nanoparticles' uptake (e.g., surface polishing or filling by nanoparticles resulting in a smoother topology, heterogeneous adhesion of the nanoparticles yielding a rougher surface, nanoparticles sliding at the interface), then the observed δf and $\delta(Q^{-1})$ shifts would reflect details of the underlying physical mechanisms. If the adsorbed film slips on the QCM surface in a response to the oscillatory motion, and/or slippage occurs at the boundary of the film with the surrounding liquid, the magnitude of the frequency shift δf_{film} will be lower than 544 Hz—the value estimated for the rigidly attached film under a no-slip contact with the surrounding fluid. These interfacial phenomena will also be reflected in the QCM's quality factor, Q, and the motional resistance, R, since the friction associated with the oscillatory motion is manifested in the quality factor. Therefore, while the exact details of the complex solid–liquid–nanoparticle interface may be unknown, changes in the motional resistance of the QCM reflect outright the frictional resistance forces at the interface and, in particular, whether the combined effect makes it easier or more difficult for the interfacial motion to occur.

Frequency shifts due to changes in temperature of the crystal are expected to be very minimal for the present work because of a prolonged equilibration of all the components with the environment and performing all the measurements at a constant room temperature. The nanoparticle suspension was placed close to the cell with DI water for sufficiently long time before the mixing in order to minimize temperature changes inside the cell upon the NP injection.

2.4 Atomic Force Microscope Characterizations of Surface Topology

Surface topology characterizations of the QCM sample sensing electrodes were performed using an atomic force microscope (AFM) (MFP 3D, Asylum Research, an Oxford Instruments Company, Santa Barbara, CA). Silicon tips were used to image the surfaces in a tapping mode in air. 1024 × 1024 images were recorded with a speed of 1 line per second. Height profiles of the surfaces recorded as $h = h(x_i,y_i)$ were quantified by the root mean square (rms) roughness value [18] $\sigma = \left(\frac{\sum\{h(x_i,y_i)-\bar{h}\}^2}{n-1}\right)^{1/2}$. The rms roughness is dependent on the size of the area sampled. For a self-affine fractal surface, the rms roughness increases with the lateral length of the sampled area as $\sigma \propto L^H$, where H is the roughness exponent whose value lies between 0 and 1. Then, $D = 3 - H$ gives the fractal dimension of the surface whose value is between 2 and 3. $D = 2$ implies a perfect 2D surface, while D higher than 2 indicates surfaces with more texture with deviation from a 2D plane. Typically, engineered surfaces have fractal characteristics with the value of D between 2 and 2.3, the lower limit being exclusive. Self-affine surfaces have an upper horizontal

cutoff length [the lateral correlation length (ξ)] above which the rms roughness saturates toward a value so-called saturated rms roughness (σ_s) and no longer exhibits the fractal scaling. The surface roughness parameters (D, σ_s and ξ) were obtained from the log(σ) versus log(scan size) plot method as described by Krim et al. [19, 20].

A log–log plot of rms roughness versus scan size of a gold surface and its surface morphology are shown in Fig. 2. The slope of the initial linear fit portion of the curve gives the roughness exponent (H), and an exponential fit for the longer length scale gives the asymptotic value of the rms roughness, i.e., the saturated rms roughness (σ_s). The lateral length where the linear fit intersects the saturated rms roughness is the correlation length (ξ). Previously, a detailed comparison of the results obtained by this method to several other techniques yielded the roughness parameters within the experimental error of each other [20].

The QCM gold surface electrodes were examined in advance of the exposure to water and after 1 and 24 h of QCM surface exposure to SiO_2 nano-suspensions. The observed values of D, σ_s and ξ were compared before and after the exposure to assess any polishing or roughening effects. AFM scans after the exposure revealed some NPs being sparsely adhered to the surface. Because such NPs would change the surface roughness parameters, such images were discarded and only the images without NPs were analyzed.

3 Results

3.1 Tribological Properties of SiO_2 Nanoparticles Interacting with a Gold Surface

The change in frequency f and motional resistance R of a QCM with a gold surface electrode in the course of NP experiments are plotted in Fig. 3 relative to their corresponding initial values in air (f_{air}, R_{air}). Upon the initial immersion of QCM in DI water, the shifts in f and R were $\delta f = -728$ Hz and $\delta R = 315\ \Omega$, respectively. Addition of SiO_2 nanoparticles directly to water resulted in further shifts of $\delta f = -30$ Hz and $\delta R = -4.6\ \Omega$ and a slow drift.

Figure 4 shows the responses of QCM in water to the addition of nanoparticles in different concentrations. The error bars for 1.5 wt% concentration represent the standard error from four independent measurements. The f and R shifts shown in Fig. 4 are measured 10 min after the addition of nanoparticles. These responses (δf and δR) were observed to have slow drifts. For example, in Fig. 3, a negative slope of f versus time was observed. We observed similar evolutions in all the runs with only some minor deviations. It is clear from Fig. 4 that the maximal decrease in R is achieved at 1.5 wt% suggesting this to be the optimal concentration for the reductions in shear.

For QCM, a decrease in R is proportional to a decrease in the inverse quality factor. Thus, the observed trends imply that the addition of NPs increased the oscillator Q-value by lowering the energy dissipation associated with resistance to shear motion at the solid–liquid interface. As discussed above, these QCM responses reflect characteristic properties of the solid–liquid–nanoparticle interface. A part of these effects could be attributed to changes in viscosity and density of the solution upon an addition of nanoparticles. But this could not be the only source for the QCM responses because any changes in density and viscosity are expected to move f and R in the opposite directions [c.f. Eqs. (1) and (2)], which is not what was observed (Figs. 3, 4). The magnitude of δf for all the nanoparticle concentrations studied is small compared to the predicted δf [calculated using Eq. (3)] for a rigidly attached nanoparticle monolayer. This reveals that the SiO_2 NPs could not make the complete coverage of the surface electrode and also infer the occurrence of a slip at the interface. The observed decrease in the energy dissipation further corroborated the possibility of a slippage at the

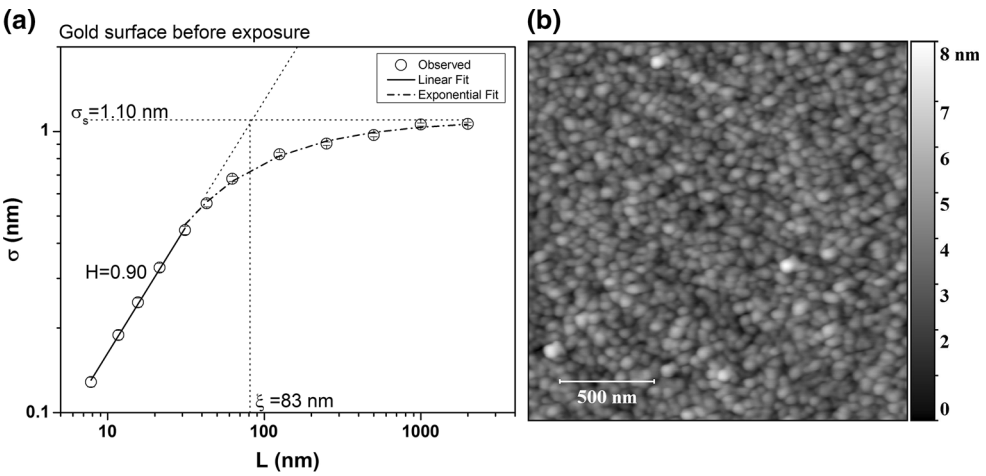

Fig. 2 **a** Calculation of roughness parameters from experimental AFM data and **b** AFM image of gold surface. See text for further detail

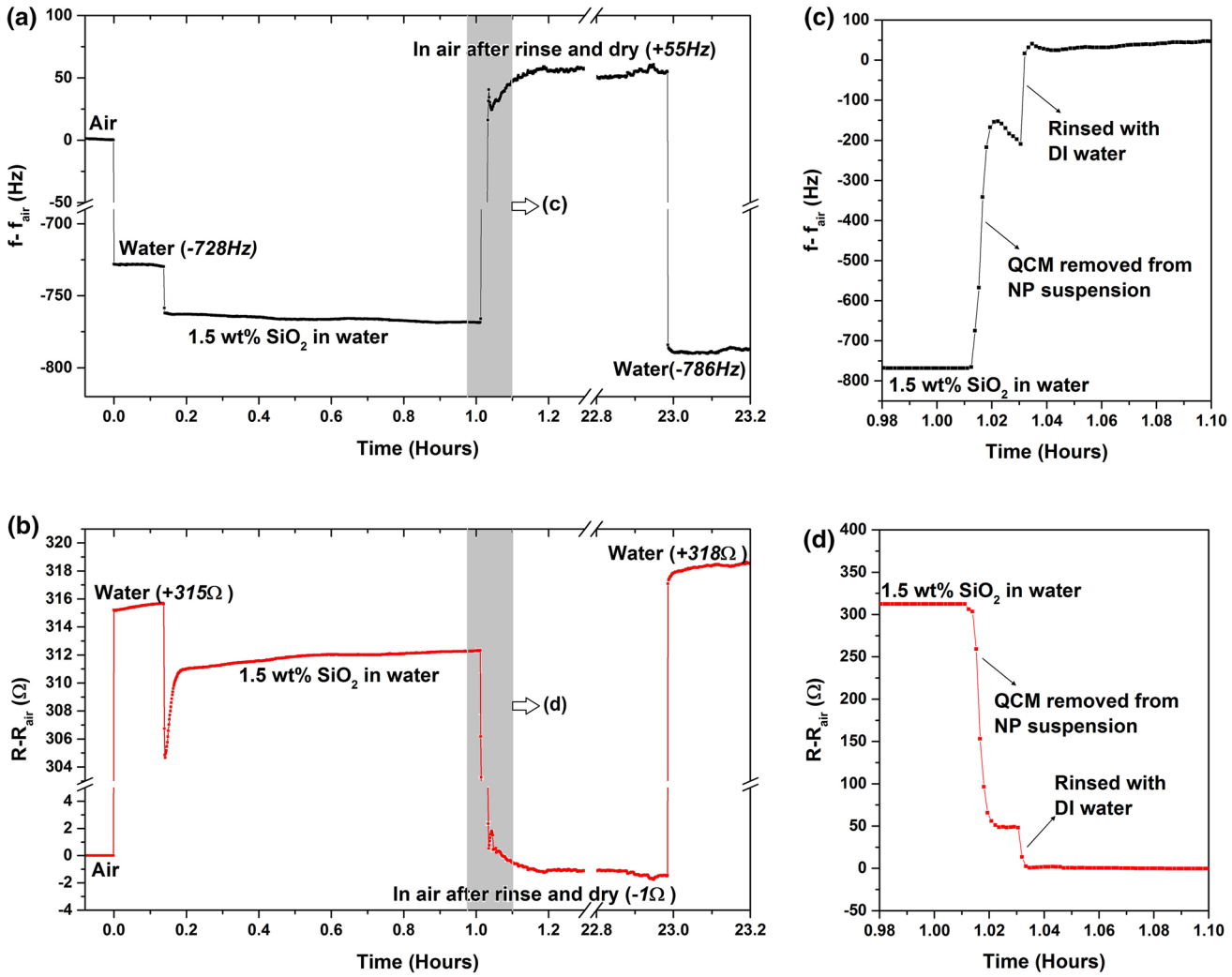

Fig. 3 Frequency (**a**) and motional resistance (**b**) response of a QCM with gold surface electrodes initially in air followed by immersion in DI water, introduction of SiO_2 nanoparticles with final concentration of 1.5 wt%, QCM removed from the nanoparticle suspension, rinsing with DI water and drying in ambient air with a consequent re-immersion in pure water. The time intervals of **a** and **b** highlighted in *gray* are expanded as **c** and **d**, respectively, to provide a detailed view

interface making it easier for the QCM to oscillate in the NP solution compared to DI water.

To examine the nature of bonding of SiO_2 NPs to the gold electrode QCM surface, the QCM was removed from the NP suspension and then rinsed with DI water and allowed to dry in ambient air. The data corresponding to the rinsing procedure is depicted in the expanded view portions (c) and (d) of Fig. 3. Immediately after removing the QCM from the NP suspension, its frequency remained lower and the resistance remained higher than the initial values in air. This is attributable to some of NPs remaining on the surface. The consequent rinsing of QCM with DI water resulted in a frequency increase to a level higher than the initial frequency before the experiment, but the motional resistance of the QCM dropped back close to its initial value in air. This increase in f is observed to be in the range of 30–70 Hz for the concentrations of NP studied and corresponds to 0.53–1.24 μg/cm^2 mass removal from the electrode surface. These observations imply not only a weak adhesion of NPs with the surface but also a removal of the material from it. This observation inferred that the δf upon an addition of NP to water (shown in Figs. 3a and 4a) is mainly caused by the physisorbed NPs on the surface with a thin coverage together with the effect of an increase in density and viscosity of the NP suspension. We note also that subsequent examination of the electrode surface with AFM revealed only sparse islands of NPs with the overall surface coverage less than a few %. It is further important to note that the δf in Fig. 4a does not increase monotonically with the increasing concentration of NP as expected from these two effects. The frequency shift δf reaches the maximum at NP concentration of 1.25 wt% and drops for

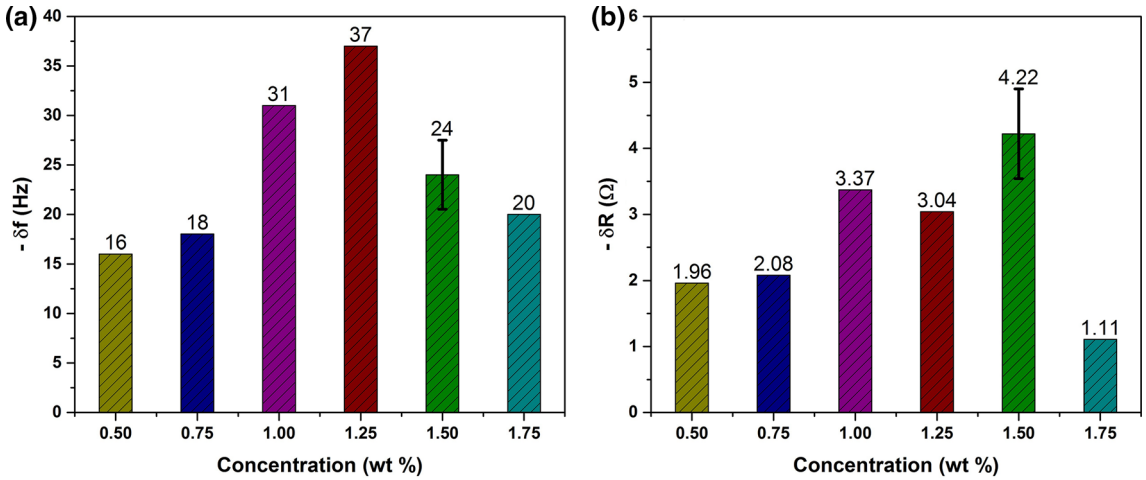

Fig. 4 Shifts in frequency (**a**) and motional resistance (**b**) of a QCM with gold surface electrodes versus concentration of SiO_2 nanoparticles in water. All the shifts were measured after 10 min of exposure to the nanoparticles w.r.t. their corresponding values in water

higher concentrations. This is a strong evidence of slippage at the boundary, which is ultimately supported by a decrease in motional resistance of the QCM with the addition of NP (Fig. 4b). The slip at the interface partially decouples the liquid from the oscillating surface that results in a decrease in the resistance to the shear motion as well as an effective mass loading on the surface. Together, these effects produce an increase in f and a decrease in R of the QCM [21]. Finally, the observed f and R responses of QCM to the addition of NPs to water are the combined effect of an increase in density and viscosity of the NP suspension, physical adsorption of NPs on the QCM surface, and the slippage at the solid–liquid–nanoparticle interfaces. While the first and third effects cause the shifts on R in the opposite directions, the observed negative shifts implied that the slippage at the interface is strong enough to overcome an increased viscosity and density of the liquid for the lubrication effect. The optimal effect of NP was observed for the concentration of 1.5 wt% at which the maximum reduction in energy dissipation of the QCM occurred.

The observed removal of mass from the QCM surface could arise from either polishing of "hilltops" or erosion of the "valleys" on the surface by the NPs subsequently changing the surface morphology. In order to explore whether the surface roughness was increasing or decreasing, the QCM crystal was cleaned and then analyzed by AFM as described in the Methods section. The AFM roughness measurement is presented in Sect. 3.2. An alternate straightforward method of assessing the change in morphology of QCM surface is by immersing the QCM in the DI water again and comparing the f and R shifts to their respective values for initial immersion in DI water, as shown in Fig. 3. It has been established that a QCM surface with higher roughness produces greater shifts in f and R [13–16]. In Fig. 3, the shifts in f and R for the second immersion of QCM in DI water are, respectively, −841 Hz and 319 Ω. Both changes are higher in magnitude than the corresponding values (−728 Hz and 315 Ω) for the initial immersion. Though minor variations in these values were observed between the runs for different concentration and four individual runs for 1.5 wt%, all of them followed the same general trend. This trend is consistent with an increase in the roughness of the QCM surface electrode [13–16] due to the exposure to nanoparticles. These observations are also in a full agreement with the AFM roughness measurement described in Sect. 3.2.

Previously, a molecular dynamics simulation (MD) study [22] of functionalized SiO_2 NPs in a solution concluded that these nanoparticles are loosely bound to the surface and sometimes even have oscillations at the surface depending on their interaction energies. The latter interactions are a manifestation of the size, surface coating, and the zeta potential of these nanoparticles. It was also revealed that these NPs need to have some separation at the surface because their mutual interactions and the interaction with the surface are the dominant contact and short-range hydrodynamic forces [22]. Also from a classical electrostatic model, placing an electrical charge regardless of its sign near a metal (conductive) surface would be equivalent of having an image charge of an opposite sign from the other side of the plane. This would result in electrostatic attraction of a charged particle to the surface. However, these charged NPs could not be packed closely to each other because of an electrostatic repulsion between the like-charged particles. This would again explain the observed incomplete coverage at the surface. During the AFM imaging, it was observed that a few nanoparticles embedded to the surface are rather sparsely. Some NPs at the lower end of the observed zeta potential range resemble

closer to uncharged particles with a distinctive property of exhibiting forced oscillation [22]. These individual NPs having distinctive oscillation frequency on the surface when coupled with the QCM constituted a two-body spring system [23] with a normal mode oscillation that they are evidently oscillating together with no relative motion. But, very few NPs meet this criterion and embed themselves on the surface, as observed during the AFM imaging. The majority of loosely bound NPs may roll and/or slip on the surface depending on their kinetic and interaction energies. The stabilization of NPs near a surface would create an effective surface charge and repulsive forces between the surface-stabilized NPs and those in solution. So, the latter NPs will be sliding due to an electrostatic repulsion and drag the surrounding liquid that will be also sliding. We suggest that these repulsive forces could be the origin of the NP lubrication effect, which would likely be a concentration-dependent phenomenon. This explanation (cf. Fig. 5) involving the occurrence of slippage at the interface is consistent with the observations detailed here and also those reported earlier [7, 8, 22]. A minimum NP concentration is required to establish a surface layer because at low concentrations the interaction between NPs may not be sufficient to overcome the thermal motion. And again, a very high concentration is not advantageous because it would eventually increase the effective viscosity and increase friction.

3.2 AFM Characterization of QCM Electrode Surfaces

Figure 6a, b shows the rms roughness versus scan size (in log–log scale) of the gold surface electrode before and after 24-h exposure to NP suspension and water, respectively. Each data point is an average of measurements taken over multiple locations on the surface, and the error bars represent the standard error on these averages. They are smaller than the size of the symbols in Fig. 6. Since the amplitude of mechanical oscillations of QCM reaches its maximum at the electrode center, the AFM images were taken from the center region.

The calculated roughness parameters summarized in Table 2 show clearly that the fractal dimension and the correlation length of the surface do not change significantly. This inferred that the texture of the surface was not altered by the nanoparticles. However, the rms roughness of the surface measurably increased by about 13–17% after exposing the electrode to SiO_2 NPs for 1 and 24 h, respectively. This suggested that the SiO_2 nanoparticles were making the surface rougher without changing its texture, with much of the evolution happening during the first hour of the exposure. This behavior is consistent with erosion of the "valleys" rather than polishing of "hilltops" and suggests a wear process associated with a rubbing motion of the nanoparticles located in such regions of the surface. In contrast, the exposure to water resulted in an increase in the rms roughness only at lateral length scales below about 40 nm. The observed values of rms roughness before and after the exposure above these length scales are within the experimental error of each other, as displayed in Fig. 6b.

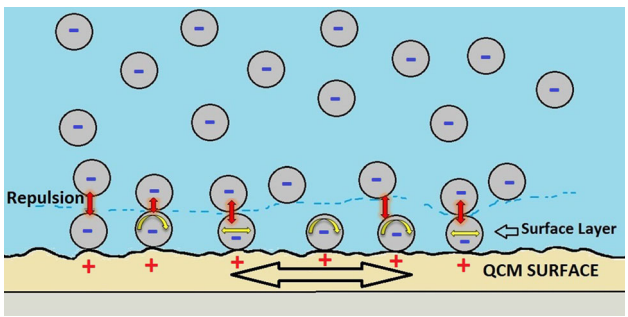

Fig. 5 A proposed mechanism of a slippage at a solid–liquid–nanoparticle interface. The majority of the nanoparticles are loosely bound to the surface and roll and/or slide on the surface, while very few are rigidly adhered. The second layer of the nanoparticles constitutes the contact layer of the bulk liquid and slips on the top of surface layer, while the repulsive forces between the individual nanoparticles provide for the observed lubrication effect

4 Discussion

Although the proposed mechanism predicts the same tribological behavior for the NPs with opposite charges, it is to bear in mind that the behavior of the opposite charges near a surface might change if the surface is charged [24, 25]. It has been reported that [4] the tribological effects were highly sensitive to the sign of the nanodiamonds' (ND) electrical charge: Negatively (positively) charged particles exhibited weaker (stronger) adhesion on gold surface. Positively charged particles consistently increased friction at the solid–liquid interface, while negatively charged particles of comparable size were observed to decrease interfacial friction. A possible explanation was that the gold surface could be also slightly charged as a function of pH, and, particularly, in alkaline range of our measurements. With this surface charge present, the NPs with opposite charges will have different interactions with the surface. The negatively charged particles will have some electrostatic repulsion between the negatively charged groups on Au surface and negatively charged NPs. But there should still be the attractive interaction from the image charge. Again, this would be consistent with a sparse NPs surface coverage and effective increase in the effective negative potential from those stabilized particles. But, a

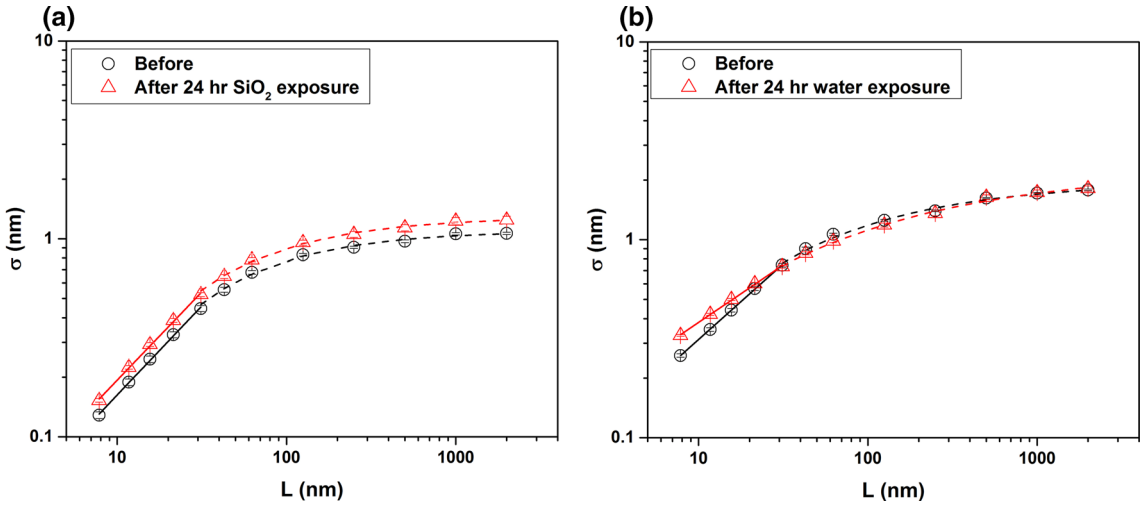

Fig. 6 Log–log plot of rms roughness versus scan size for gold surface electrodes before and after 24 h of exposure to **a** SiO_2 NPs and **b** DI water. The *solid* and *broken lines*, respectively, represent the least squares fits for the linear initial sections and the exponential further sections of the experimental curves. Exposure to SiO_2 NPs results in an increase in the surface roughness at all length scales measured, while the exposure to water alone has no observable effect at length scales above 20 nm

Table 2 Roughness parameters of gold surface electrode before and after 1 and 24 h of exposure to SiO_2 nanoparticle suspension

	Fractal dimension (D)	Saturated rms roughness (σ_s) (nm)	Lateral correlation length (ξ) (nm)
Before	2.1	1.10	83 ± 4
After 1 h	2.1	1.24	75 ± 4
After 24 h	2.1	1.29	84 ± 4

positively charged particle might have behaved in a different manner. This also raises an additional interesting question of the applicability of continuum electrostatic models to charged NPs interacting with the surface.

The SiO_2 NPs' effect of a reduction in shear resistance to the motion of a QCM in water observed in this study is analogous to the other tribological observations made using various tribological techniques. The lubrication effect maximizes at a certain concentration of NPs and then reduces back with a further increase in the concentration [6, 8]. The optimal concentration of SiO_2 NPs reported in various studies [6, 8] is different, however. This is likely attributed to different size and surface properties of NPs and the properties of the tribological interface. One study [26] reported that these NPs were not observed to improve the performance of the base lubricant for the concentrations below 0.2 wt%, while another study [8] with different base lubricant and surface modification testified their lubrication effect for concentration as small as 0.1 wt%. For the QCM technique employed here, the reduction in shear resistance was observed for NP concentrations higher than 0.5 wt% with an optimal effect at ca. 1.5 wt%. The variations in the results between different tribological observations are due to the dissimilar experimental conditions such as different base lubricants, surface modifications of NPs and even the variation in materials used for the test. All of these parameters influence the interaction of SiO_2 NPs to the surface and the mutual interactions between the NPs. An interesting future direction would be to perform QCM studies with stainless steel coated surfaces and surface-modified SiO_2 NPs to find the direct correlation with the tribological studies [5–8] carried out under similar conditions. In particular, given that the QCM measures a reduction in viscous shear forces at the solid liquid interface, it would be interesting to observe the size of the impact of this hydrodynamic component of friction on the overall friction levels measured in macroscale settings. The surface modification of NPs can significantly affect lubrication by altering their mutual interaction, zeta potential (or charge) in the liquid and also the interactions with the contacting surfaces. If the surface-modified functional groups have a tendency to attach to the surface, then it may help to establish the NP layer on the surface sooner and the lubrication effect can be observed at lower concentrations. Despite the variabilities in the results of various studies, all of these suggested the common ground for the NP lubrication effect to be the formation of a NP surface layer (or NP film as reported in some studies) and their impacts on the mating surfaces or interactions with the NPs in the bulk liquid.

Further informative studies could be performed by varying the pH of the liquid to include both acidic and alkaline range so as to vary the charge on NPs and the surface(s) and/or explore whether the interfacial shear could be tuned by application of an external electrical field. Such charge-dependent NP lubrication would be analogous

to electrokinetic phenomenon [27] and/or electroosmotic flow effects [28].

5 Conclusions

The nano-tribological properties of gold surfaces immersed in aqueous suspensions of SiO_2 nanoparticles were examined with QCM and AFM. The principle observations and conclusions are as follows:

- The SiO_2 nanoparticles were found to reduce the resistance to shear motion at the QCM's solid–liquid interface.
- The SiO_2 nanoparticles were not observed to rigidly attach to the surfaces, for example, as a chemisorbed layer.
- The effect was observed to be concentration dependent, with 1.5 wt% yielding a maximum reduction in shear at the solid–liquid–nanoparticle interface.
- The nanoparticles were observed to remove the electrode material from the surface and slightly increase the overall roughness with the major change happening within the first hour of the exposure.
- A suggested electrokinetic mechanism for these observations is that the loosely bound nanoparticles roll and/or slide on the surface, while upper layers of nanoparticles slips over the surface layer because of the repulsive electrostatic forces between the individual particles.

Overall, this study provides an insight into the complex interface of solid, liquid and nanoparticles at a nanometer scale and suggests a mechanism that has been overlooked, to date, for the tribological properties of nanoparticle suspensions.

Acknowledgements This work was supported by National Science Foundation Award Number DMR1535082. SEM studies were performed at the Analytical Instrumentation Facility (AIF) at North Carolina State University, which is supported by the State of North Carolina and the National Science Foundation (Award Number ECCS-1542015). The AIF is a member of the North Carolina Research Triangle Nanotechnology Network (RTNN), a site in the National Nanotechnology Coordinated Infrastructure (NNCI).

References

1. Spikes, H.: Friction modifier additives. Tribol. Lett. (2015). doi:10.1007/s11249-015-0589-z
2. Dai, W., Kheireddin, B., Gao, H., Liang, H.: Roles of nanoparticles in oil lubrication. Tribol. Int. **102**, 88–98 (2016)
3. Krim, J.: Friction and energy dissipation mechanisms in adsorbed molecules and molecularly thin films. Adv. Phys. **61**(3), 155–323 (2012)
4. Liu, Z., Leininger, D., Koolivand, A., Smirnov, A.I., Shenderova, O., Brenner, D.W., Krim, J.: Tribological properties of nanodiamonds in aqueous suspensions: effect of the surface charge. RSC Adv. **5**(96), 78933–78940 (2015)
5. Liu, X., Xu, N., Li, W., Zhang, M., Chen, L., Lou, W., Wang, X.: Exploring the effect of nanoparticle size on the tribological properties of SiO_2/polyalkylene glycol nanofluid under different lubrication conditions. Tribol. Int. **109**, 467–472 (2017)
6. Jiao, D., Zheng, S., Wang, Y., Guan, R., Cao, B.: The tribology properties of alumina/silica composite nanoparticles as lubricant additives. Appl. Surf. Sci. **257**, 5720–5725 (2011)
7. Gorbunova, T.I., Zapevalov, A.Y., Beketov, I.V.: Preparation and antifrictional properties of surface modified hybrid fluorine-containing silica particles. Appl. Surf. Sci. **326**, 19–26 (2015)
8. Bao, Y.Y., Sun, J.L., Kong, L.H.: Tribological properties and lubricating mechanism of SiO_2 nanoparticles in water-based fluid. IOP Conf. Ser. Mater. Sci. Eng. **182**(1), 012025 (2017)
9. Sorensen, C.M.: The mobility of fractal aggregates: a review. Aerosol Sci. Technol. **45**(7), 765–779 (2011)
10. Stanford Research System: QCM 100 Quartz Crystal Microbalance Analog Controller—QCM 25 Crystal Oscillator. Stanford Research Systems Inc, California (2002)
11. Kanazawa, K.K., Gordon, J.G.: Frequency of a quartz microbalance in contact with liquid. Anal. Chem. Acta **175**, 99–105 (1985)
12. Martin, S.J., Granstaff, V.E., Frye, G.C.: Characterization of a quartz crystal microbalance with simultaneous mass and liquid loading. Anal. Chem. **63**, 2272–2281 (1991)
13. Martin, S.J., Frye, G.C., Ricco, A.J., Senturia, S.D.: Effects of surface roughness on the response of a thickness-shear mode resonator in liquids. Anal. Chem. **65**, 2910–2922 (1993)
14. Urbakh, M., Daikhin, L.: Influence of the surface morphology on the quartz crystal microbalance response in a fluid. Langmuir **10**(8), 2836–2841 (1994)
15. Daikhin, L., Gileadi, E., Katz, G., Tsionsky, V., Urbakh, M., Zagidulin, D.: Influence of roughness on the admittance of the quartz crystal microbalance immersed in liquids. Anal. Chem. **74**(3), 554–561 (2002)
16. Acharya, B., Sidheswaran, M.A., Yungk, R., Krim, J.: Quartz crystal microbalance apparatus for study of viscous liquids at high temperatures. Rev. Sci. Instrum. **88**(2), 025112 (2017)
17. Sauerbrey, G.: Verwendung von Schwingquarzen zur Wägung dünner Schichten und zur Mikrowägung. Z. Phys. A Hadrons Nucl. **155**(2), 206–222 (1959)
18. Krim, J., Palasantzas, G.: Experimental observations of self-affine scaling and kinetic roughening at submicron lengthscales. Int. J. Mod. Phys. B **09**, 599 (1995)
19. Krim, J., Heyvaert, I., Van Haesendonck, C., Bruynseraede, Y.: Scanning tunneling microscopy observation of self-affine fractal roughness in ion-bombarded film surfaces. Phys. Rev. Lett. **70**(1), 57 (1993)
20. Palasantzas, G., Krim, J.: Scanning tunneling microscopy study of the thick film limit of kinetic roughening. Phys. Rev. Lett. **73**(26), 3564 (1994)
21. Urbakh, M., Tsionsky, V., Gileadi, E., Daikhin, L.: Probing the solid/liquid interface with the quartz crystal microbalance. In: Steinem, C., Janshoff, A. (eds.) Piezoelectric Sensors, vol. 5, pp. 111–149. Springer, Berlin, Heidelberg (2006)
22. Lane, J.M.D., Ismail, A.E., Chandross, M., Lorenz, C.D., Grest, G.S.: Forces between functionalized silica nanoparticles in solution. Phys. Rev. E **79**(5), 050501 (2009)
23. Dultsev, F.N., Kolosovsky, E.A.: QCM model as a system of two elastically bound weights. Sens Actuators B **242**, 965–968 (2017)
24. Curtis, C.K., Krim, J.: Comparative study of the distinguishing characteristics of effective eco-friendly lubricants comprised of water-based nanodiamond suspensions. Submitted to Beilstein Journal of Nanotechnology (under review)

25. Jing, D., Pan, Y., Wang, X.: The effect of the electrical double layer on hydrodynamic lubrication: a non-monotonic trend with increasing zeta potential. Beilstein J. Nanotechnol. **8**, 1515–1522 (2017). doi:10.3762/bjnano.8.152
26. Tucker, Z.: The performance of translucent silicon-oxide nanoparticle lubricant additives. Tribol. Lubr. Technol. **73**(4), 32–34 (2017)
27. Schoch, R.B., Han, J., Renaud, P.: Transport phenomena in nanofluidics. Rev. Mod. Phys. **80**(3), 839 (2008)
28. Bocquet, L., Barrat, J.L.: Flow boundary conditions from nano-to micro-scales. Soft Matter **3**(6), 685–693 (2007)